Vol. 60: 199–213, 2014
doi: 10.3354/cr01234

CLIMATE RESEARCH
Clim Res

Published August 5

FREE ACCESS

Climate projections for Vietnam based on regional climate models

Thanh Ngo-Duc[1,*], Chanh Kieu[2], Marcus Thatcher[3], Dzung Nguyen-Le[4], Tan Phan-Van[1]

[1]Department of Meteorology, Hanoi College of Science, Vietnam National University, Hanoi 10000, Vietnam
[2]Laboratory for Weather and Climate Forecasting, Hanoi College of Science, Vietnam National University, Hanoi 10000, Vietnam
[3]CSIRO Marine and Atmospheric Research, PMB 1, Aspendale, Victoria 3195, Australia
[4]Department of Geography, Tokyo Metropolitan University, Hachioji 192-0397, Japan

ABSTRACT: This study uses an ensemble of regional climate models (RCMs) to simulate and project the climate of Vietnam. Outputs of 3 global climate models are dynamically downscaled using 3 RCMs. Experiments are performed for a baseline period from 1980 to 1999 and for a future projection from 2000 to 2050 with the A1B emission scenario. Verifications against observations at 61 selected meteorological stations in the region show that an ensemble mean of the 3 RCMs outperforms the individual RCM in representing the climatological mean state, and reasonably captures some extreme climate indices such as the annual maximum daily temperature (TXx), the annual minimum daily temperature (TNn), and the annual maximum 1 d precipitation (RX1day). Future ensemble projections of the temperature, precipitation, and 3 different extreme indices are then evaluated. The simulations predict the 2 m air temperature over Vietnam to significantly increase in both the near future 2011–2030 and middle-future 2031–2050 periods compared to the baseline period. The temperature trend tends to be positive and significant over the whole Vietnam for the spring, summer and fall periods, whereas it is insignificant in the north central region during winter. The highest increase of ~0.5°C decade^{-1} appears to be pronounced in summer. For precipitation, future changes vary depending on regions and seasons, with the most significant increasing trend over the coastal plain of Central Vietnam, particularly during the winter monsoon season. Under the global warming scenario A1B, TXx and TNn show a significant increase, with the highest rate in the northern and central highlands regions of Vietnam. The extreme precipitation RX1day indices show increasing trends for the coastal zone in the south central region of Vietnam, suggesting more severe water-related disasters in this region in the future.

KEY WORDS: Dynamical downscaling · Multi-model approach · Climate extreme indices · Vietnam

1. INTRODUCTION

Reliable information about future climate conditions for specific regional locations under different climate change scenarios is of great importance to stakeholders, decision makers and other societal entities. These climate projections are particularly essential for Vietnam in preparation and adaptation because of its high vulnerability to future climate changes (UNFCCC 2007). Different techniques have been used to capture climatological characteristics at the regional scale such as statistical downscaling (Wilby et al. 1998, 2004), high resolution atmospheric global climate models (GCMs) (Cubasch et al. 1995, Kitoh et al. 2009), or dynamical downscaling using regional climate models (RCMs) (e.g. Giorgi & Mearns 1999, Phan et al. 2009, Ho et al. 2011). Despite extensive research and international colla-

*Corresponding author: ngoducthanh@vnu.edu.vn

boration, numerous uncertainties related to future greenhouse gas emissions, natural climate variability, model parameterizations and inadequate representations of the initial/lateral boundary conditions in the climate model system, however, put a strong limit on our current capability in obtaining robust trends of future climate in a specific region.

Of all approaches, GCMs are currently considered the most useful tool in climate change research because of their versatility in integrating different climate scenarios. Due to coarse spatial resolutions of the global models that are typically larger than 100 km in the horizontal dimension, dynamical downscaling of GCM outputs using RCMs has recently become a practical approach to the study of present day and future climate (Solomon et al. 2007). A vast number of previous studies have demonstrated the capability of RCMs in reproducing fine-scale features for different regional climates (e.g. Tadross et al. 2005, Dash et al. 2006, Gao et al. 2006, Seth et al. 2007, Phan et al. 2009). For example, Dash et al. (2006) showed the suitability of an RCM in simulating the Indian summer monsoon circulation features and associated rainfall; Gao et al. (2006) used an RCM to show that simulated precipitation over the East Asian region can be improved as the horizontal resolution is increased, and Phan et al. (2009) studied RCM-simulated rainfall and temperature over Vietnam during the 1991–2000 period and found that model outputs were in good agreement with observations.

The well-established capability of RCMs in reproducing present climate conditions suggests that RCMs would be useful tools to provide future regional climate information. Because of inherent deficiencies in RCMs related to imperfect treatment of physical representations using parameterizations, model configuration, or initial and boundary conditions, multiple sources of uncertainties nevertheless exist in any projection of future climate (e.g. Castro et al. 2005, Rockel et al. 2008). The most common solution to reduce such model uncertainties is to combine results from a range of models, the so-called multi-model ensemble approach (e.g. Christensen & Christensen 2007, Déqué et al. 2007, Jacob et al. 2007, Tebaldi & Knutti 2007, Van der Linden & Mitchell 2009, Liu et al. 2011, Iizumi et al. 2012). Following this approach, the Coordinated Regional Climate Downscaling Experiment – East Asia (CORDEX-EAS: http://cordex-ea.climate.go.kr/), which aimed at improving coordination of international efforts, was initiated for the East Asia region. However, studies with direct applications of this multiple model approach for projecting future climate in Vietnam and the surrounding Southeast Asian regions appear to be limited to date.

Of specific interest to historical climate change in Vietnam and surrounding regions are studies of Manton et al. (2001), Takahashi (2011), Kajikawa et al. (2012). Endo et al. (2009) found that heavy precipitation increases in southern Vietnam but decreases in northern Vietnam during the 1950s to early 2000s. Using RegCM3 to study future climate for 7 climatic sub-regions in Vietnam, Ho et al. (2011) found that the number of hot summer days (cold winter nights) tends to increase (decrease) as a consequence of global warming. They also projected that heavy rainfall events largely increase over southcentral Vietnam, whereas those extreme events are stable or decrease for most other sub-regions. Using the statistical downscaling approach, the Ministry of Natural Resources and Environment (MONRE) of Vietnam published several official scenarios of climate change and sea level rise for Vietnam (MONRE of Vietnam 2009). According to this official report, the annual mean temperature in Vietnam is projected to increase by about 2.3°C by the late 21st century for the medium B2 SRES scenario (Special Report on Emissions Scenarios) (Nakicenovic et al. 2000); total annual and rainy season rainfall may also increase while rainfall tends to decrease in dry seasons as compared to the baseline period of 1980–1999.

This study is our first attempt in combining information from several different RCMs driven by different GCMs to evaluate future climate conditions for Vietnam. We will focus mainly on assessment of the performances of the RCMs for the present day climate and discuss about the derived future trends of temperature, precipitation, and several extreme indices in the region.

2. NUMERICAL EXPERIMENTS AND DATA

2.1. Numerical experiments

In this study, 3 experiments using 3 RCMs to respectively downscale outputs of 3 GCMs were conducted. Note that each RCM was paired with a host GCM, producing 3 projections. The 3 RCMs are the Conformal Cubic Atmospheric Model (CCAM) (McGregor 2005, McGregor & Dix 2008), the Regional Climate Model Version 3 (RegCM3) (Giorgi & Mearns 1999), and the Regional Model (REMO) (Jacob 2001). The 3 GCMs comprise the CCAM model (global runs), the Community Climate System

Model version 3 model (CCSM3) (Collins et al. 2005), and the European Centre Hamburg Model 5th generation model (ECHAM5) (Roeckner et al. 2003) coupled to the Max Planck Institute for Meteorology Ocean Model (MPIOM) (Jungclaus et al. 2006). CCAM, CCSM3 and ECHAM5 are the host GCMs of the CCAM, RegCM3, and REMO RCMs, respectively. Two periods were selected for each simulation: (1) a baseline period from 1980 to 1999 during which the 3 GCMs were driven by observed atmospheric greenhouse gas and aerosol concentrations, and (2) a near future period (2000–2050) during which the A1B emission scenario was used (Nakicenovic et al. 2000). The common domain for all experiments covers an area with longitude varying from 100° to 120° E and latitude from 5° to 25° N. Since CCAM was not coupled to an ocean model, sea surface temperatures (SSTs) in the global climate simulation were based on output from the Geophysical Fluid Dynamics Laboratory Coupled Model (GFDL CM2.1, Delworth et al. 2006). Average SST biases were calculated for each month over the period 1971–2000 and then used to bias correct the GFDL CM2.1 SSTs for the present and future climate simulations (Nguyen et al. 2011). In this way, the mean SST bias is corrected, while retaining the amplitude of SST variability and other climate change signals. For RegCM3 and REMO, the SSTs simulated by the coupled models CCSM3 and ECHAM5-MPIOM, respectively, were used without any bias correction. Table 1 summarizes the domain information, lateral boundary conditions and physical parameterizations used by each RCM.

Given outputs from the 3 RCMs, an arithmetic ensemble mean is composed for each climate variable (hereafter referred to as the ENS product). As shown in previous studies, such an ensemble mean can have a significant advantage over a single model projection as it can help to offset some individual model biases. This advantage is mostly manifested in cases where the model bias has a Gaussian distribution so that negative and positive biases can offset each other. In reality, models exhibit very different

Table 1. Information about model domain, physics, and boundary condition assigned in each individual regional climate model (RCM)

	CCAM	RegCM3	REMO
Grid size	C80 (80 × 80 × 6 grids) with a regional focus, 25 km	142 × 103 grids, 36 km	145 × 97 grids, 36 km
Number of vertical levels	18	18	20
Model domain	100–120° E, 5–25° N (extracted from the global domain)	85–131° E, 5° S–27° N	85–131° E, 5° S–27° N
Radiation parameterization	Diurnally varying GFDL parameterization (Schwarzkopf & Fels 1991)	CCM3 (Kiehl et al. 1996)	Morcrette (1989), Giorgetta & Wild (1995)
Convective parameterization	Mass-flux cumulus convection scheme (McGregor 2003)	Grell scheme (Grell 1993) with the Arakawa-Schubert closure assumption (Arakawa & Schubert 1974)	Mass flux (Tiedtke 1989), CAPE closure (Nordeng 1994)
Planetary boundary layer parameterization	Based on the local Richardson number (McGregor et al. 1993) and the Holtslag & Boville (1993) non-local vertical mixing	Holtslag PBL (Holtslag et al. 1990)	Louis (1979)
Land surface parameterization	Canopy scheme (Gordon et al. 2002)	BATS (Dickinson et al. 1993)	Hagemann & Dümenil Gates (2003), ECHAM4 (Roeckner et al. 1996)
Sea surface temperature (SST)	GFDL CM2.1 bias corrected SST, monthly updated	CCSM3 SST, monthly updated	ECHAM5-MPIOM SST, monthly updated
Initial and lateral boundary data	CCAM-global	CCSM3	ECHAM5
Lateral boundary condition	Updated every 6 h	Updated every 6 h	Updated every 6 h

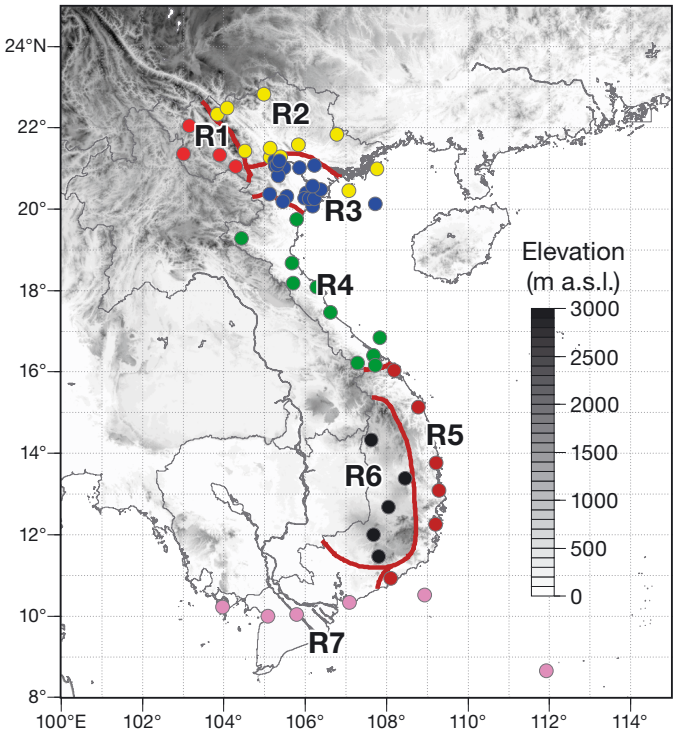

Fig. 1. The ENS domain, 7 sub-climatic regions of Vietnam (R1→R7) and locations of the 61 meteorological stations used in the study. Each station is represented by one dot colored according to the sub-region that it belongs to. m a.s.l.: m above sea level

behaviors and could have better skill in particular areas, time periods, or meteorological fields. For this kind of situation, a weighted ensemble mean can be formulated to take into account the advantageous points of each individual model. Such a weighted ensemble approach, however, requires substantial evaluations in the model space that we are currently not able to afford. Thus, the arithmetic ensemble mean approach will be used in this preliminary assessment of model projections. In Section 3, we will evaluate the CCAM, RegCM3, REMO and ENS simulations against observations.

2.2. Observed data

To evaluate the RCMs simulations, the daily observed temperature and precipitation time series from 61 local meteorological stations in Vietnam have been collected for the baseline period of 1980–1999 (Fig. 1). Missing data were assigned a value of –99.0. Fig. 1 also represents the 7 sub-climatic regions of Vietnam (R1→R7) that were identified in Phan et al. (2009) and Ho et al. (2011).

2.3. Climate extreme indices

For climate projections, changes in extreme events are important because of their profound impacts on nature and society. To identify an extreme event, different indices have been defined and used. The joint WMO Commission for Climatology (CCI)/World Climate Research Programme (WCRP) Climate Variability and Predictability (CLIVAR) project's Expert Team on Climate Change Detection, Monitoring and Indices (ETCCDMI) recommend 27 core extreme climate indices based on daily temperature values or daily precipitation amount. The definitions of the indices and the formulas for calculating them are available from http://cccma.seos.uvic.ca/ETCCDMI.

In this study, we wish to examine 8 extreme indices of which 5 indices (TXx, TNn, RX1day, CDD, CWD – see definitions in Table 2) are recommended by ETCCDMI, and the other 3 indices (Tx35, T2m15, R50)

Table 2. The 8 extreme climate indices used in this study. The indices are calculated on a yearly basis

	Extreme indices	Definition	Unit	Recommended by
1	Tx35	Annual count of hot days when daily maximum temperature (Tx) ≥ 35°C	d	VNHMS
2	T2m15	Annual count of cold days when daily mean temperature (Tm) ≤ 15°C	d	VNHMS
3	TXx	Annual maximum value of daily maximum temperature	°C	ETCCDMI
4	TNn	Annual minimum value of daily minimum temperature	°C	ETCCDMI
5	R50	Annual count of days when precipitation (R) ≥ 50 mm d^{-1}	d	VNHMS
6	RX1day	Annual maximum 1 d precipitation	mm	ETCCDMI
7	CDD	Annual maximum length of dry spell, maximum number of consecutive days with R < 1 mm d^{-1}	d	ETCCDMI
8	CWD	Annual maximum length of wet spell, maximum number of consecutive days with R ≥ 1 mm d^{-1}	d	ETCCDMI

are the extreme thresholds currently used by the National Hydro-Meteorological Service of Vietnam (VNHMS) (Ho et al. 2011). The 8 indices were individually calculated for each model and averaged for the ENS product.

3. MODEL PERFORMANCES IN THE BASELINE PERIOD

To examine how each individual RCM captures the past climate during the baseline period (1980–1999), Fig. 2 compares the baseline average air temperature and wind fields at 850hPa for June-July-August (JJA) and December-January-February (DJF). Overall, all 3 RCMs show spatial distributions of the zonal wind and temperature consistent with both the GCM inputs and the ERA40 reanalysis data. Specifically, CCAM RCM and REMO reproduce well the wind fields on the large scale similar to what is achieved with the GCMs, whereas RegCM3 shows rather weaker wind speed with a more southward wind component over the southern part of Vietnam in JJA as compared to its global CCSM boundary. Although CCAM RCM reproduces well its boundary temperature field, it overestimates temperature as compared to the ERA reanalysis data, particularly in the north and central regions of Vietnam. In contrast, RegCM3 clearly shows a cold bias in the simulated temperature, and REMO has a warm bias in both JJA and DJF as compared to their driving GCM boundaries and the ERA-40 reanalysis. We notice that part of the bias in RCMs is inherent from the driving GCM bias (e.g. the CCAM GCM bias, Fig. 2). The downscaling process with RCMs could introduce some further differences, but this indicates that a proper choice of GCM could play a significant role in enhancing the downscaling products.

Since the ERA-40 reanalysis data do not capture the detailed local spatial characteristics of the cli-

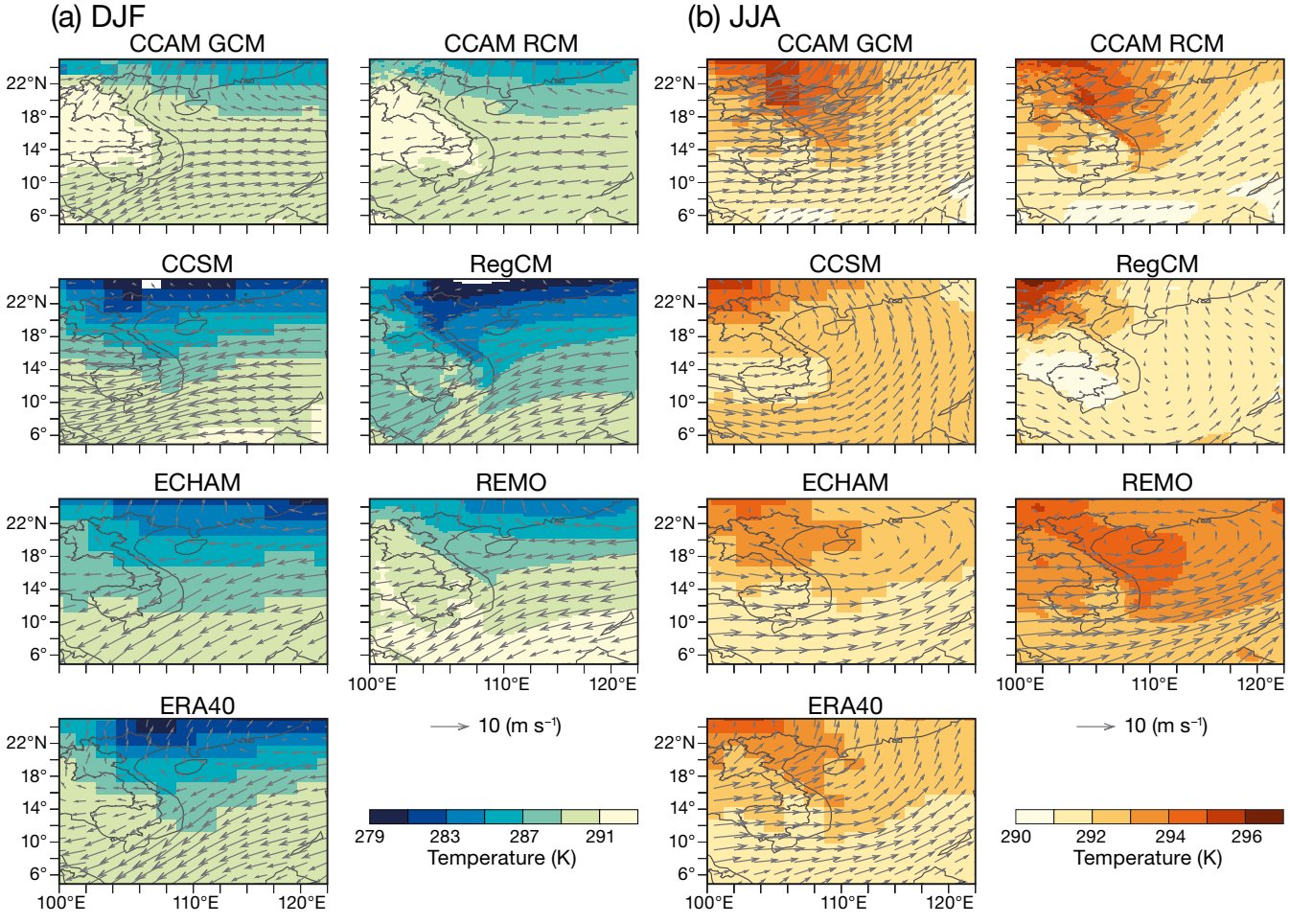

Fig. 2. 1980–1999 mean temperature at 850 hPa from (left) the GCMs and the ERA40 reanalysis data and (right) the RCMs in (a) winter and (b) summer. Wind speed and direction at 850 hPa are superimposed (arrows)

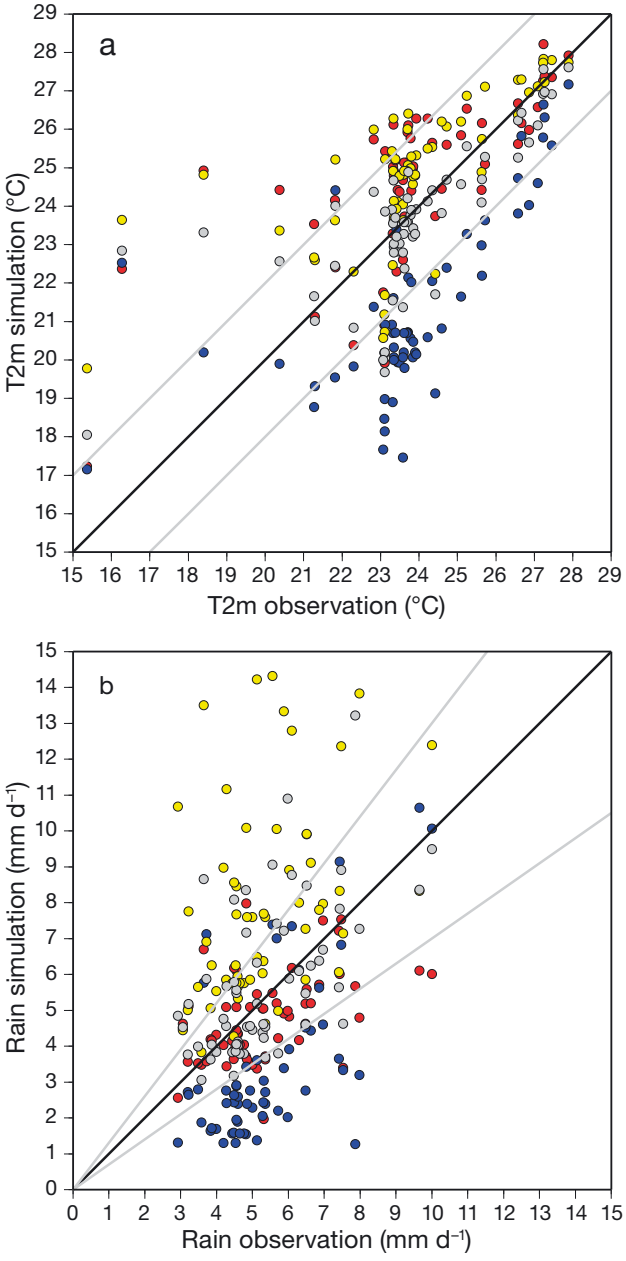

Fig. 3. Scatter diagrams of simulated (a) 2 m temperature (T2m), and (b) precipitation compared to observations at 61 stations: CCAM (red), RegCM3 (blue), REMO (yellow) and the mean product (ENS; grey). Grey lines: 'good' simulation range of ±2°C for temperature and ±30% for precipitation from observations

mate, Fig. 3 provides more specific verifications of the RCM outputs against local observations at 61 meteorological stations over Vietnam (cf. Fig. 1). For each station, the annual mean values averaged for the baseline period of the nearest land-grid point of the RCM outputs are used to directly compare with the observations. Similar to that seen in Fig. 2, the 2 m temperature (T2m) simulated by RegCM3 is systematically underestimated, but it appears to be overestimated by CCAM and REMO at most of the stations. The cold bias produced by the RegCM3 model was also identified in previous studies (e.g. Rauscher et al. 2007, Seth et al. 2007, Phan et al. 2009, Ho et al. 2011). Given such mixed bias behaviors among the RCMs, we note that the ENS product yields a much more consistent distribution with most of the interpolated values distributed within ±2°C of the observed values (Fig. 3a).

RegCM3 appears to systematically underestimate accumulated precipitation, with most of the values clustering near the tail of the diagram (~4 to 5 mm d^{-1}), while it is generally overestimated by REMO, especially at the larger tail of the scattering diagram (~7 to 10 mm d^{-1}; Fig. 3b). The CCAM model represents observed precipitation fairly well, as most of the station points concentrate along the expected line for perfect simulations. Similar to T2m, the ensemble combination of all 3 models again agrees generally better with observations than each individual model, with most of the simulated values concentrated along the diagonal line, indicating the superior performance of the multiple model ensemble during the baseline period.

As mentioned in Section 2.2, it is important to study changes of extreme events because of their profound impacts on nature and society. Extreme events are identified by extreme values, which are normally located in the tails of the probability distribution of a relevant climatic variable.

Fig. 4 shows how the 3 RCMs and the ENS product represent T2m, precipitation and the 8 extreme indices for the baseline period, based on correlation, mean bias and root mean square error (RMSE) between the simulated values and the observations at the 61 stations used in the study. The mean bias and RMSE are respectively normalized by the observation mean and the range of the observed data, making them non-dimensionless.

Fig. 4a shows that the ENS product tends to produce a better correlation with the observed values compared to those of the 3 RCMs, except for CDD and RX1day. The correlations are relatively low (<0.5) for Tx35, CDD, and R50, indicating that the models and the ENS product cannot capture well the spatial pattern of those extreme indices over the 61 stations of Vietnam. Fig. 4c shows that ENS generally exhibits better (i.e. smaller) normalized root mean square errors (NRMSE) compared to the 3 RCMs, except for CWD and precipitation.

For the normalized mean biases (NMB) of the temperature indices, the systematic biases identified for

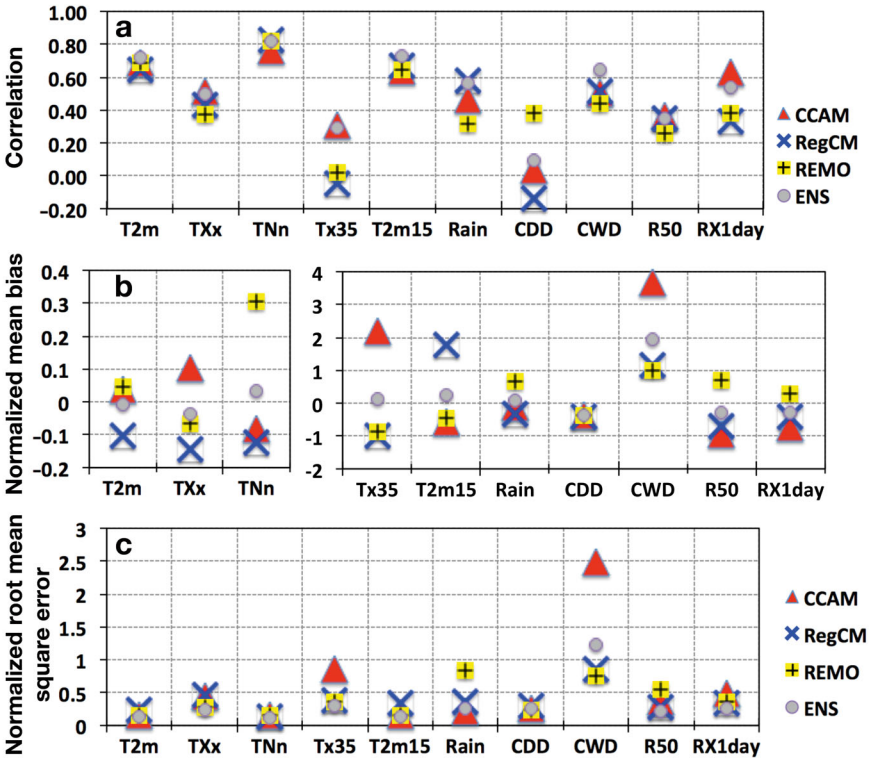

Fig. 4. Statistics of simulated 2m-temperature, precipitation and the 8 extreme indices in comparison with the observations at 61 stations

the climatological T2m are not reproduced for the extreme values (Fig. 4b). For example, REMO TXx and CCAM TNn are underestimated whereas REMO T2m and CCAM T2m are generally overestimated. Among the temperature extreme indices, the NMBs of TXx and TNn are the closest to zero, indicating that TXx and TNn are relatively well reproduced by the RCMs. Nevertheless, REMO and RegCM3 systematically underestimate Txx, whereas CCAM overestimates it. For TNn, while CCAM and RegCM3 generally show the negative biases of TNn over the 61 stations, REMO has relatively large positive biases. ENS is most consistent with the observed TXx and Tnn, as most of the station points are distributed within ±2°C of the observed values (not shown).

As a result of the systematic biases of the RCMs in representing T2m, several absolute extreme thresholds, such as Tx35 and T2m15 (Fig. 4b), are not sufficiently represented by the models. 35°C is a too low a threshold of maximum daily temperature to characterize a hot day for CCAM whereas it is an extremely high threshold for REMO and RegCM3. Similarly, 15°C is a too high a threshold to characterize a cold day for RegCM3 whereas the same threshold is too low for REMO and RegCM3. Consequently, Tx35 and T2m15 NMBs of the RCMs are out of the [–0.5, 0.5] range, indicating that the models have large biases (>50%) compared to observations. The poor performance of the RCMs in representing Tx35 and T2m15 NMBs suggests that those indices may not be fully appropriate to diagnose the future climatic changes in the study area from these RCMs without some kind of statistical correction (e.g. Piani et al. 2010), which is beyond the scope of the present study.

For the precipitation extreme indices, all 3 RCMs poorly represent the R50, CDD, and CWD indices as compared to observations. For example, R50 is largely underestimated in CCAM and RegCM3, but largely overestimated in REMO (Fig. 4b). Similarly, the maximum observed CWD is around 20 d, whereas the simulated CWD can reach 40 d or more in the models (not shown), resulting in very high values of NMBs (Fig. 4b) and NRMSE (Fig. 4c). This indicates that the models can easily satisfy the wet day threshold ($R \geq 1$ mm d^{-1}). Consequently, CDD is generally underestimated by the models, and has low correlation with the observations. Similar to the temperature extreme indices, the absolute threshold is an inappropriate choice, and results in poor RCM performance in representing the respective precipitation indices.

For RX1day, the models can partially represent the spatial distribution with some systematic biases. REMO overestimates RX1day whereas RegCM3 and CCAM underestimate this index. The positive/negative biases of the simulated RX1day follow those of the simulated climatological precipitation for REMO and RegCM3, respectively (Fig. 3b). However, while CCAM fairly well represents the observed mean precipitation in terms of NMB and NRMSE, the CCAM annual maximum daily precipitation is significantly underestimated, implying that the good correspondence in the mean statistics between CCAM and the observation does not ensure a good correspondence in the tail of the distribution function. This is in agreement with Iizumi et al. (2011), who showed that unlike climatological mean states, averaging of precipitation extreme values over Japan from multiple models does not always outperform the single best model.

To better quantify the performance of each experiment, we define 2 criteria, T2 and P30, for selecting the experiments that better simulate mean T2m, precipitation and extreme values. If *obs* is defined as an observed quantity, criterion T2 is then satisfied when the simulated temperature variables consisting of T2m, TXx and TNn are within a range of *obs* ± 2°C. Similarly, P30 is satisfied when the simulated mean precipitation, or the remaining extreme indices (Table 3), are within the range of *obs* ± 30%. If a simulation of a variable at one station is further defined as a 'good' one when the corresponding criterion (T2 or P30) is satisfied, it is possible to collect the number of 'good' stations for each experiment for that variable.

Comparison of each individual RCM and the ENS product in Table 3 shows that the ensemble mean is closest to the observations for the mean T2m and precipitation. Except for CCAM that has slightly more stations satisfying the P30 criteria (45 points), ENS possesses the largest number of stations that satisfy the T2 (50 'good' stations), and P30 (43 'good' stations) criterion. Although the number of 'good' stations is significantly reduced for the extreme indices, ENS still has the highest number of 'good' stations with 33, 24 and 30 cases for TXx, TNn, and RX1day (Table 3), respectively. Note, however, that scattering diagrams similar to Fig. 3 (but not shown here) indicate a poor performance of the RCMs and the ENS product in representing the T2m15 (20 cases) and CDD (34 cases). This is particularly apparent at the larger tail of the diagrams. For Tx35, R50, and CWD, the number of 'good' stations for ENS is low, resulting directly from the poor performance of each individual experiment.

Further analysis of Figs. 3 & 4 shows that the simulated temperature, precipitation, and their respective extreme indices differ substantially among the 3 RCMs. Such differences can be attributed to the different model parameterizations or to insufficient representation of the initial and boundary conditions. As an illustration, Fig. 5 plots the differences in SST between the CCAM-global, CCSM3 and ECHAM5 boundary conditions and the observation-based Hadley Centre Sea Ice and Sea Surface Temperature data set (HadISST) (Rayner et al. 2003). As the mean SST bias of CCAM-global (i.e. GFDL CM2.1) was corrected, a high similarity between CCAM-SST and HadISST is found. Fig. 5 shows that the CCSM3 SST is significantly lower than the observed SST. In particular, the colder CCSM3 SST regions are located in the northeast of the northern mainland and in the southwest of southern Vietnam, where northeast and southeast winds are prevailing during the winter and summer monsoon seasons, respectively. The colder SST would partly explain the negative bias of the simulated surface temperature by RegCM3 in the baseline period (Fig. 4b). This colder SST also results in weaker convective activities, which tend to decrease evaporation over the open ocean. As a result, less moisture is advected to the mainland, partly explaining the large underestimation of the precipitation in the RegCM3 model (Fig. 4b). ECHAM5 also has a cold SST bias (Fig. 5), but the REMO outputs forced by ECHAM5 showed warmer and wetter biases (Fig. 3). A possible reason is that ECHAM5 SST is not as cold as that of CCSM3, and the warm characteristic of REMO (Fig. 2) can cancel out the cold biases originating from the ocean.

Table 3. Number of 'good' stations among the total 61 stations corresponding to the T2 and P30 criteria

	Criterion	CCAM	RegCM3	REMO	ENS
T2m	T2	45	17	47	50
Precipitation	P30	45	13	24	43
TXx	T2	21	5	18	33
TNn	T2	19	21	23	24
Tx35	P30	6	3	6	5
T2m15	P30	14	12	17	20
RX1day	P30	0	10	30	30
R50	P30	0	8	25	15
CDD	P30	38	33	34	34
CWD	P30	0	11	8	0

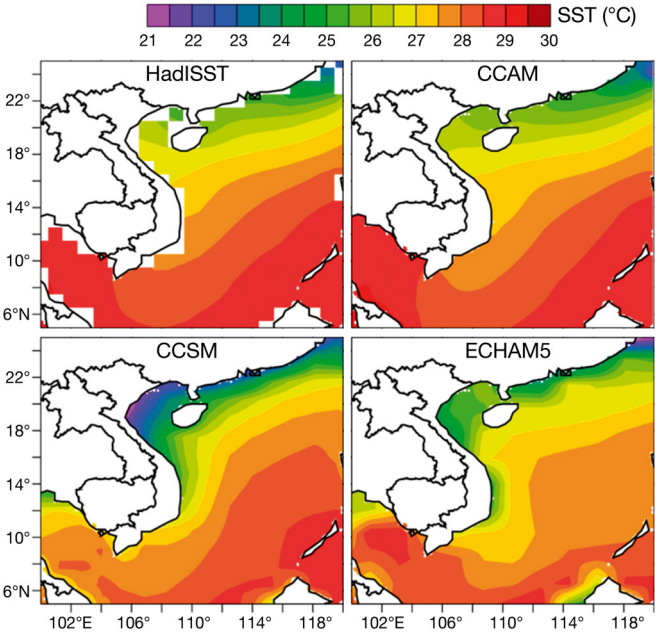

Fig. 5. 1980–1999 average SST from the observation-based HadISST, and the CCAM-global, CCSM3 and ECHAM5 boundary conditions

4. COMBINING FUTURE CLIMATE CONDITIONS

As shown in Section 3, ENS has consistent advantages in representing the mean statistics and certain extreme indices. In this section, we will use this ensemble approach to examine potential climate projections of the 2 m temperature (T2m), precipitation, and some of their derived extreme climate indices for the future period of 2000–2050 with the A1B emission scenario. To be specific, the differences between the near-future period 2011–2030 (hereinafter referred to as NF), the middle-future period 2031–2050 (hereinafter referred to as MF) and the baseline period 1980–1999 (hereinafter referred to as BS) are first examined. As a result, some systematic biases of the models detected in Section 3 can be alleviated in the differences between the future and the baseline periods. The Student's paired *t*-test is used to compute the statistical significance of the differences. Then, future projections of the variables are characterized by trend slopes, which are estimated using the non-parametric Sen's slope method (Sen 1968). Briefly, the Sen's slope of a data series (x_1, x_2, …, x_n), where x_i represents the value at time i, is the median of the series composed of n(n – 1)/2 elements $\{\frac{x_j - x_k}{j - k}$, $k = 1, 2, \ldots, n - 1; j > k\}$. A positive value of the Sen's slope indicates an upward trend, whereas a negative value indicates a downward trend. To assess the significance of trends, the non-parametric Mann-Kendall (Kendall 1975) statistical test is used.

4.1. Future temperature and precipitation

Fig. 6 displays the differences of T2m between NF, MF and BS. The angled-grid patterns over each figure represent areas of statistical significance at the 90% level. The thin-black contours represent 'consistent' areas where the change in T2m for ENS, CCAM, RegCM3 and REMO have the same sign (not necessarily significant). Thus the contours indicate where all the experiments are in agreement for the

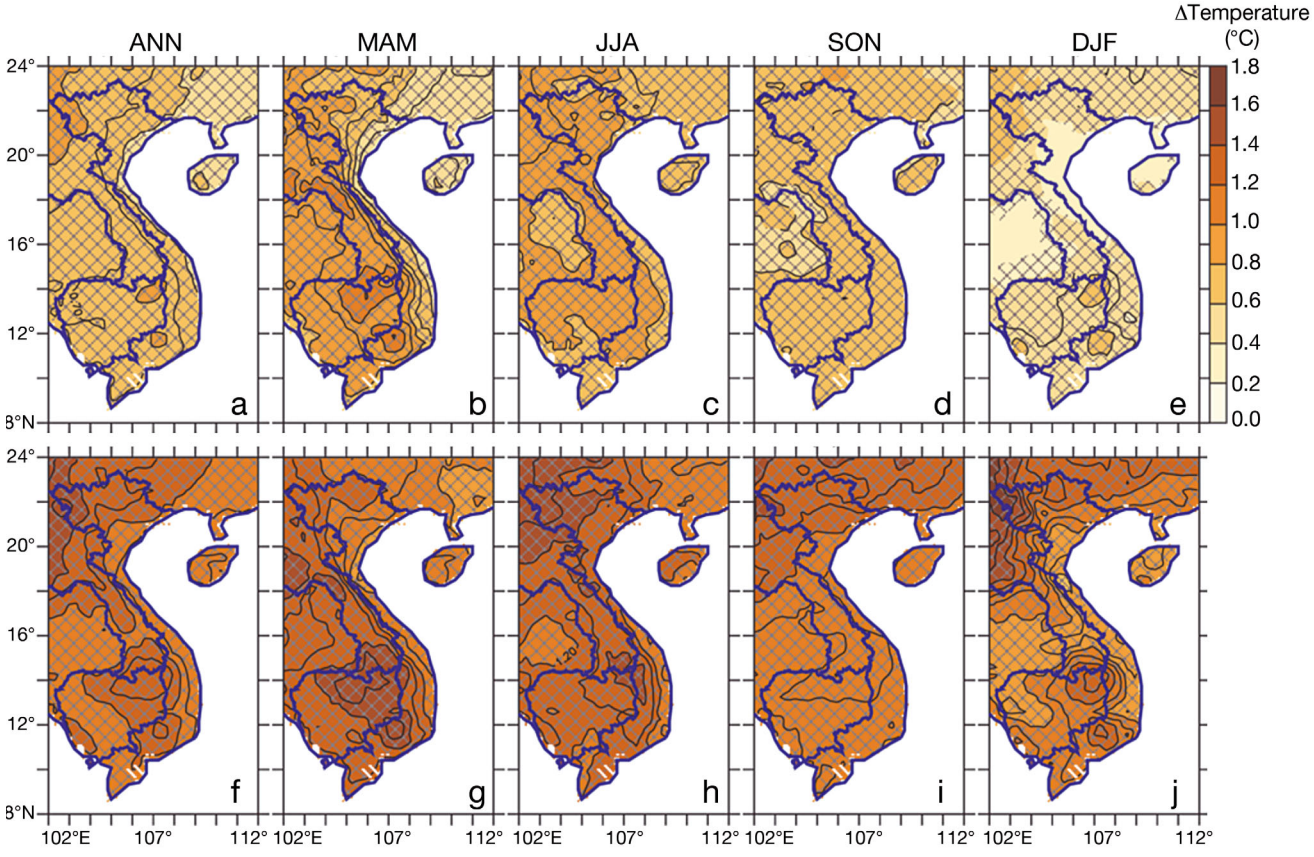

Fig. 6. Differences of ENS 2 m temperature between (a–e) 2011–2030 and 1980–1999, and (f–j) 2031–2050 and 1980–1999 for (a,f) annual, (b,g) spring, (c,h) summer, (d,i) autumn, and (e,j) winter means. The angled-grid patterns represent areas with a 90% level of statistical significance. Thin black contours: areas where ΔTemperature for ENS, CCAM, RegCM3 and REMO has the same sign. Blue lines show international borders

direction of changes, which increase our confidence about the certainty of the obtained results.

For annual (ANN) and seasonal values (MAM, JJA, SON, and DJF for the spring, summer, autumn, and winter season, respectively), T2m significantly increases in both NF and MF compared to BS. The level of temperature increase is higher in MF than in NF. The highest increase is approximately 1.8°C during JJA MF in the northwest region of Vietnam. While the changes for all the seasons in the MF period are consistent among the models (i.e. changes in T2m for all 3 RCMs and ENS have the same sign), the changes in SON and DJF of NF temperature are inconsistent, particularly for the northern region of Vietnam.

Fig. 7 displays the projected trend of T2m for 2000–2050. For ANN, MAM and SON, the annually averaged T2m increases significantly over the entire Vietnam region, except for a small region in the north central area. The trend is larger and more consistent in the south and northwest of Vietnam. Similar to the differences between the future and baseline periods, the T2m trend is significantly and consistently positive over the whole of Vietnam in the summer. The highest increase in JJA is approximately 0.5°C decade^{-1}, located mostly in the northern region. In DJF, the T2m trend is only significant and consistent in the south. In the north central region (R4, Fig. 1), the ENS product shows a small decreasing trend. However, this trend is not consistent for the 3 RCMs.

Unlike the T2m differences, the precipitation differences (Fig. 8) vary widely, depending on regions, seasons, and future periods. A decrease in precipitation by as much as 25% can be observed in the northern regions, specifically for ANN, MAM and DJF of NF and for ANN and DJF of MF, whereas an increase by up to 15% can be seen in south central region for MF and for JJA and SON of NF. Fig. 8 also shows that the precipitation changes are insignificant at 90% confidence level for most regions and seasons, except for northern Vietnam in ANN of NF, north central Vietnam in MAM and JJA of NF, south central Vietnam in ANN, JJA and SON of MF. The models generally show their inconsistencies in the direction of precipitation changes, except for south central region in the MF period.

Regarding the trend for 2000–2050 (Fig. 9), precipitation has a slight increasing rate of 0.1 to 0.3 mm d^{-1} decade^{-1} in MAM except for a part of the North (R1, R2) and the highland regions (R6) where the ENS trend is not significant. In JJA, the trend is generally insignificant and inconsistent from the highland region northward, whereas a significant increasing trend is detected in the windward side of the mountain ranges (e.g. southwest of the highland region). This indicates that southwest summer monsoons are likely to be more active in the future. In SON, precipitation consistently increases in the south central region (R5) and in the northern part (R2). There is a significant increasing trend up to 0.5 mm d^{-1} decade^{-1} in the northwest part and up to 1 mm d^{-1} decade^{-1} in the coastal plain of central Vietnam. The consistent increasing trend in the central region remains during the winter (Fig. 9e). It should be noted that the major rainfall appears in the central part of Vietnam from September to December (Yen et al. 2011). Thus, an increasing rate of rainfall in this region could consequently lead to more rainfall-related extreme events in the future, which will be further examined in the next sub-section. For ANN, a signif-

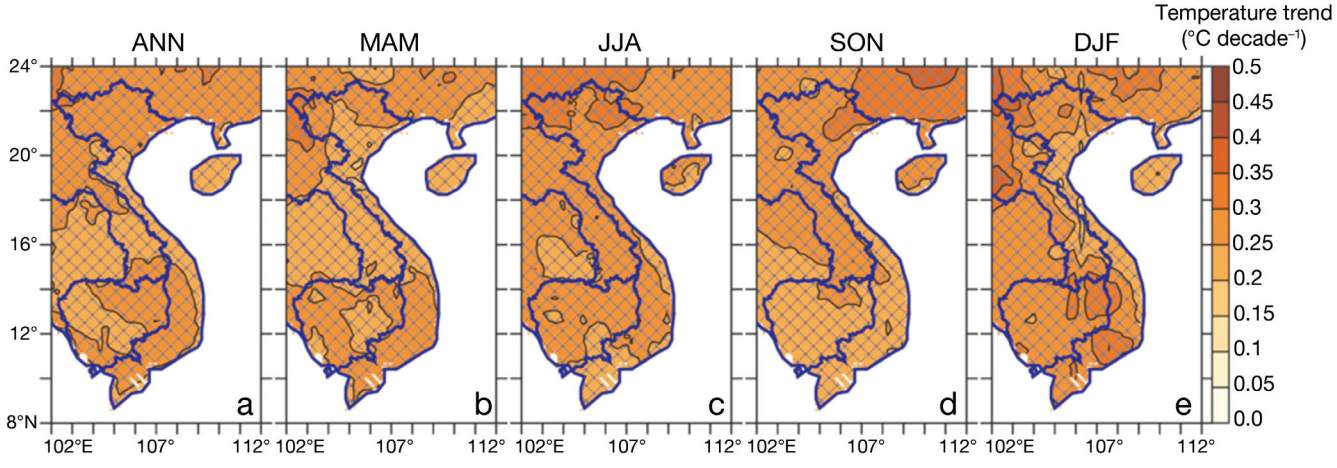

Fig. 7. 2000–2050 trend of ENS 2 m temperature (shading areas) for (a) annual, (b) spring, (c) summer, (d) autumn, and (e) winter means. The angled-grid patterns represent areas of 90% level of significance. Thin black contours: areas where ENS, CCAM, RegCM3 and REMO have the same trend-sign. Blue lines show international borders

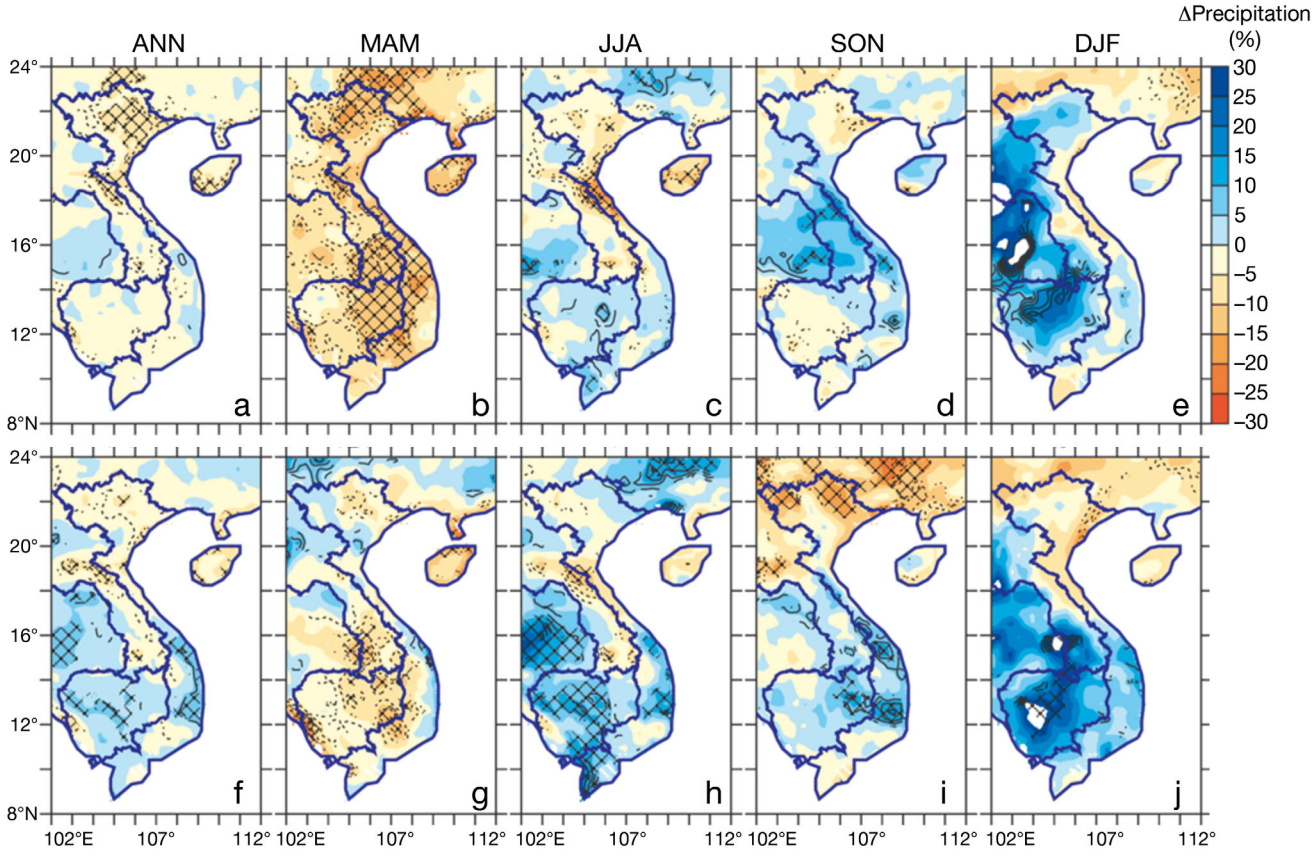

Fig. 8. Same as Fig. 6 but for precipitation

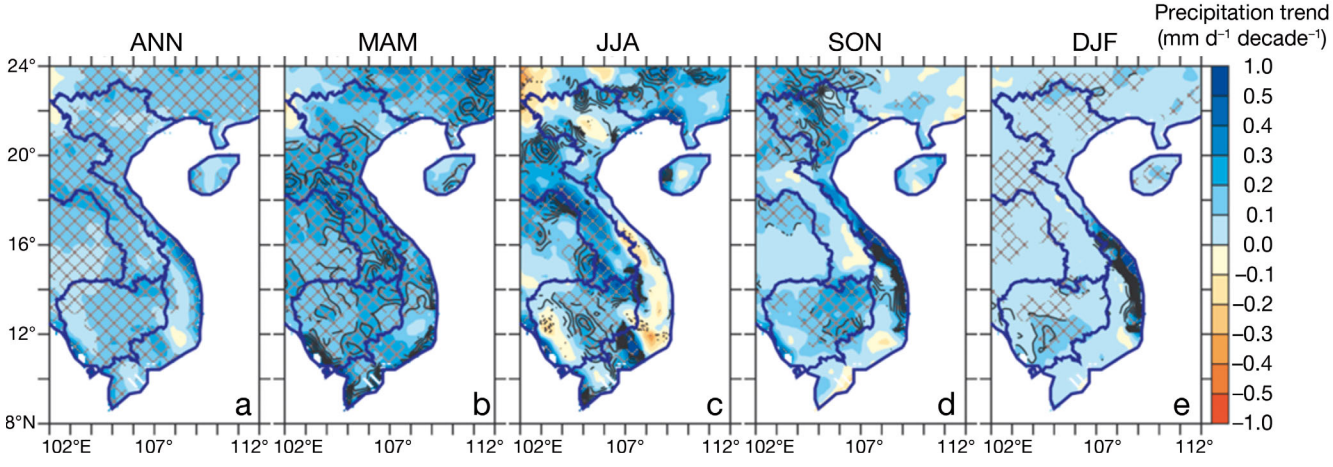

Fig. 9. Same as Fig. 7 but for precipitation

icant and positive trend is identified except for the highland region, and a small area in the southern part of Vietnam. The trend is largest (up to 0.5 mm d^{-1} $decade^{-1}$) in the coastal plain of central Vietnam, which is mainly due to the SON and DJF precipitation increase. However, the 3 RCMs and ENS do not show the same trend-sign for the ANN product over the study area; thus, the ANN precipitation trend is not consistent.

4.2. Changes in climate extreme events

The poor performance of the RCMs in representing the extreme indices, which are defined by absolute thresholds such as Tx35, T2m15, R50, CDD and CWD, suggest that those indices seems to be inappropriate to diagnose the future climatic changes in the study area. Therefore, we only examine the future changes and trends of the 3 indices TXx, TNn

and RX1day in Figs. 10 & 11. The changes and trends of those indices, their significance and consistency among the experiments are obtained using the same methods as applied to the T2m and precipitation.

Fig. 10 shows that TXx and TNn significantly and consistently increase in NF and MF compared with the BS period. An exception is for NF TNn, where the changes are not statistically significant in the central and northeast regions of Vietnam. TXx increases more rapidly than TNn for both NF and MF. The changes in MF can reach 1.8°C and 1.6°C for TXx and TNn, respectively, which are higher by approximately 0.2°C than those in NF. For RX1day, the ENS product shows a slight decrease in NF for almost all over Vietnam. However, ENS RX1day in MF increases by up to 10 to 20% in south central Vietnam. The ensemble RX1day changes are insignificant at the 90% confidence level for almost regions (Fig. 10c,f). The models also show their inconsistencies in the direction of RX1day changes, except for some small areas in the MF period.

Regarding the trend of the extreme indices for the period 2000–2050, Fig. 11 shows that both TXx and TNn increase consistently over Vietnam with higher increasing rate in the northern part and in the highland region. The trend can reach ~0.39°C decade^{-1} and ~0.33°C decade^{-1} for TXx and TNn, respectively. The slope of TXx is higher than that of TNn, indicating that the annual temperature range is likely to expanded in the future, particularly in northern Vietnam.

Unlike the temperature indices, the annual maximum 1 d precipitation (RX1day) mainly shows significant trends for the coastal zone in south central Vietnam (R5, cf. Fig. 11c). Here, RX1day increases by ~1 to 2.5 mm d^{-1} decade^{-1}, and its trend is also consistent. In R3 and the northern part of R4, the trend is not significant, although the 3 RCMs and their ENS products have the same trend-sign.

The increasing trend of extreme rainfall events in south central Vietnam is also reported in Ho et al. (2011), who suggested that this trend could be associated with the intensification of the number or intensity of severe tropical cyclones over the north Western Pacific basin in the future. Verification of this hypothesis would be an interesting subject for a future study. It should be noted that Ho et al. (2011) considered the same RegCM3 simulation as the one used in the present study for investigating the difference between the means of future and baseline period.

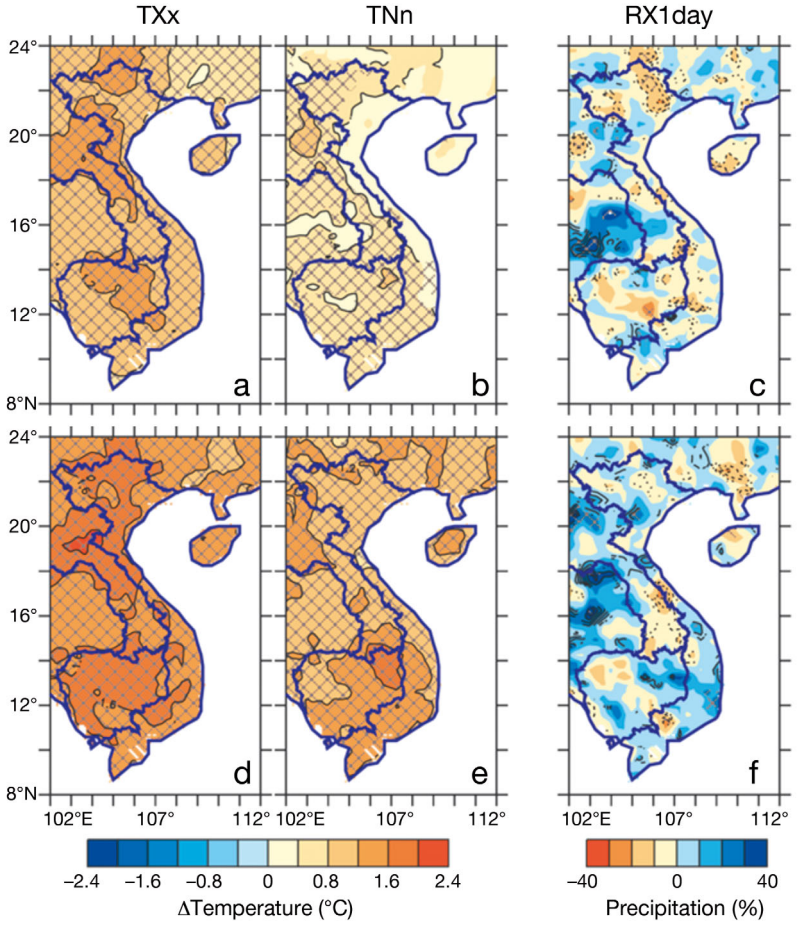

Fig. 10. Same as Fig. 6 but for annual differences in (a,d) TXx, (b,e) TNn, and (c,f) RX1day

5. CONCLUSIONS

In this study, climate change and future projection for Vietnam have been examined using a dynamical downscaling approach for 3 GCMs with 3 RCMs including the CCAM, RegCM3, and REMO models. While these regional models demonstrated their capability in capturing some of the climate characteristics along Vietnam coastal zone, there are some significant biases in each individual model that render the downscaling uncertain to some degree. Further examination of the ensemble mean of the outputs from the 3 models shows that the ensemble mean appears to outperform

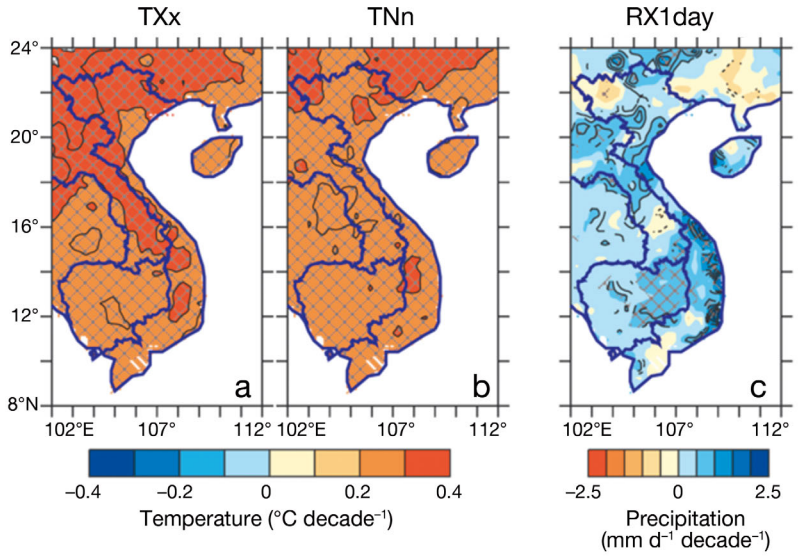

Fig. 11. Same as Fig. 7 but for annual trends in (a) TXx, (b) TNn, and (c) RX1day

the 3 RCMs in representing the climatological-mean state and some certain extreme climate indices such as TXx, TNn and RX1day.

Results for future changes in climate show that the mean temperature significantly increases in both the NF and MF periods compared to the baseline period. Temperature increase is higher in MF than in NF. The T2m trend during the period 2000–2050 is generally positive and significant over the whole Vietnam for MAM, JJA and SON, whereas it is only significant and consistent in the southern region for DJF. The highest increase (~0.5°C decade^{-1}) appears in JJA. For the extreme temperature indices, we found that as a consequence of global warming, TXx and TNn significantly increase at the highest rate in the northern and central highland regions of Vietnam.

Unlike the T2m, the mean precipitation changes vary substantially, depending on region and season. The models generally show inconsistencies in representing precipitation changes, except for south central region in the MF period. During the period 2000–2050, a positive trend is significantly identified except for the highland region and a small area in the southern part of Vietnam. The coastal area of central Vietnam has the highest increasing trend, particularly during the winter monsoon season. The annual maximum 1 d precipitation index (RX1day) shows significant and consistent increasing trends for the coastal zone in the south central region of Vietnam. This suggests more severe water-related disasters in this region in the future.

This study is our preliminary attempt to combine outputs of different RCMs for future climate projections in Vietnam. The fact that the ensemble mean outperforms any individual RCM model in representing the climatological-mean state and certain extreme indices confirms the importance of using a multi-model system for reducing inherent uncertainties of models. As the dynamical downscaling approach is time-consuming and requires extensive resources, international collaboration is thus needed. In line with the CORDEX downscaling activities, our future plan is to investigate future climate conditions based on the experiments forced with the latest GCM climate scenarios produced within the Coupled Model Intercomparison Project Phase 5 (CMIP5).

Acknowledgements. The authors thank 3 anonymous reviewers and the responsible editor, Dr. Oliver Frauenfeld, for their constructive comments and suggestions, which helped improve the manuscript greatly. This research was supported by the Vietnam Ministry of Science and Technology Foundation (DT.NCCB-DHUD.2011-G/10), the 11-P04-VIE DANIDA project, and the Vietnam National Foundation for Science and Technology Development (NAFOSTED, code: 105.06-2013.03).

LITERATURE CITED

Arakawa A, Schubert WH (1974) Interaction of a cumulus cloud ensemble with the large-scale environment. Part 1. J Atmos Sci 31:674–701

Castro CL, Pielke RA, Leoncini G (2005) Dynamical downscaling: assessment of value retained and added using the Regional Atmospheric Modeling System (RAMS). J Geophys Res 110:D05108, doi:10.1029/2004JD004721

Christensen JH, Christensen OB (2007) A summary of the PRUDENCE model projections of changes in European climate by the end of this century. Clim Change 81(Suppl 1):7–30 (Prudence Special Issue)

Collins WD, Bitz CM, Blackmon ML, Bonan GB and others (2006) The Community Climate System Model Version 3. J Clim 19:2122–2143

Cubasch U, Waszkewitz J, Hegerl G, Perlwitz J (1995) Regional climate changes as simulated in time-slice experiments. Clim Change 31:273–304

Dash SK, Shekhar MS, Singh GP (2006) Simulation of Indian summer monsoon circulation and rainfall using RegCM3. Theor Appl Climatol 86:161–172

Delworth TL, Broccoli AJ, Rosati A, Stouffer RJ and others (2006) GFDL's CM2 global coupled climate models. 1. Formulation and simulation characteristics. J Clim 19: 643–674

Déqué M, Rowell D, Lüthi D, Giorgi F and others (2007) An intercomparison of regional climate models for Europe: assessing uncertainties in model projections. Clim Change 81(Suppl 1):53–70 (Prudence Special Issue)

Dickinson RE, Henderson-Sellers A, Kennedy PJ (1993) Biosphere-Atmosphere Transfer Scheme (BATS) version 1E as coupled to the NCAR Community Climate Model. NCAR Tech Note, Natl Cent for Atmos Res, Boulder, CO

Endo N, Matsumoto J, Lwin T (2009) Trends in precipitation extremes over Southeast Asia. SOLA 5:168–171

Gao XJ, Xu Y, Zhao ZC, Pal JS, Giorgi F (2006) On the role of resolution and topography in the simulation of East Asia precipitation. Theor Appl Climatol 86:173–185

Giorgetta M, Wild M (1995) The water vapour continuum and its representation in ECHAM4. Report No. 162. Max-Planck-Institut für Meteorologie, Hamburg

Giorgi F, Mearns LO (1999) Introduction to special section: regional climate modeling revisited. J Geophys Res 104(D6):6335–6352

Gordon HB, Rotstayn LD, McGregor JL, Dix MR and others (2002) The CSIRO Mk3 climate system model. Technical Report 60, CSIRO Atmospheric Research

Grell GA (1993) Prognostic evaluation of assumptions used by cumulus parameterization. Mon Weather Rev 121: 764–787

Hagemann S, Dümenil Gates L (2003) Improving a subgrid runoff parameterization scheme for climate models by the use of high resolution data derived from satellite observations. Clim Dyn 21:349–359

Ho TMH, Phan VT, Le NQ, Nguyen QT (2011) Extreme climatic events over Vietnam from observational data and RegCM3 projections. Clim Res 49:87–100

Holtslag A, Boville B (1993) Local versus non-local boundary layer diffusion in a global climate model. J Clim 6: 1825–1842

Holtslag A, De Bruijn E, Pan HL (1990) A high resolution air mass transformation model for short-range weather forecasting. Mon Weather Rev 118:1561–1575

Iizumi T, Nishimori M, Dairaku K, Adachi SA, Yokozawa M (2011) Evaluation and intercomparison of downscaled daily precipitation indices over Japan in present-day climate: strengths and weaknesses of dynamical and bias-correction-type statistical downscaling methods. J Geol Res 116:D01111, doi:10.1029/2010JD014513

Iizumi T, Takayabu I, Dairaku K, Kusaka H and others (2012) Future change of daily precipitation indices in Japan: a stochastic weather generator-based bootstrap approach to provide probabilistic climate information. J Geophys Res 117:D11114, doi:10.1029/2011JD017197

Jacob D (2001) A note to the simulation of the annual and inter-annual variability of the water budget over the Baltic Sea drainage basin. Meteorol Atmos Phys 77:61–73

Jacob D, Bärring L, Christensen OB, Christensen JH and others (2007) An inter-comparison of regional climate models for Europe: design of the experiments and model performance. Clim Change 81(Suppl 1):31–52 (Prudence Special Issue)

Jungclaus JH, Keenlyside N, Botzet M, Haak H and others (2006) Ocean circulation and tropical variability in the coupled model ECHAM5/MPI-OM. J Clim 19:3952–3972

Kajikawa Y, Yasunari T, Yoshida S, Fujinami H (2012) Advanced Asian summer monsoon onset in recent decades. Geophys Res Lett 39:L03803, doi:10.1029-2011GL 050540

Kendall MG (1975) Rank correlation methods. Charles Griffin, London

Kiehl JT, Hack JJ, Bonan GB, Boville BA, Briegleb BP, Williamson DL, Rasch PJ (1996) Description of the NCAR Community Climate Model (CCM3). Tech Note NCAR/TN-420+STR, Boulder, CO

Kitoh A, Ose T, Kurihara K, Kusunoki S, Sugi M, KAKUSHIN Team-3 Modeling Group (2009) Projection of changes in future weather extremes using super-high-resolution global and regional atmospheric models in the KAKUSHIN Program: results of preliminary experiments. Hydro Res Lett 3:49–53

Liu CM, Wu MC, Paul S, Chen YC and others (2011) Super-ensemble of 3 RCMs for climate projection over East Asia and Taiwan. Theor Appl Climatol 103:265–278

Louis JF (1979) A parametric model of vertical eddy fluxes in the atmosphere. Boundary-Layer Meteorol 17:187–202

Manton MJ, Della-Marta PM, Haylock MR, Hennessy KJ and others (2001) Trends in extreme daily rainfall and temperature in Southeast Asia and the South Pacific: 1961–1998. Int J Climatol 21:269–284

McGregor JL (2003) A new convection scheme using a simple closure. Res Rep 93:33–36, Bureau of Meteorology Research Centre, Melbourne

McGregor JL (2005) C-CAM: geometric aspects and dynamical formulation. Tech Pap 70, CSIRO Marine and Atmospheric Research, Melbourne

McGregor JL, Dix MR (2008) An updated description of the conformalcubic atmospheric model. In: Hamilton K, Ohfuchi W (eds) High-resolution simulation of the atmosphere and ocean. Springer, New York, NY, p 51–76

McGregor JL, Gordon HB, Watterson IG, Dix MR, Rotstayn LD (1993) The CSIRO 9-level Atmospheric General Circulation Model. CSIRO Marine and Atmospheric Research Technical Report 26. www.cmar.csiro.au/e-print/open/mcgregor_1993a.pdf

Morcrette JJ (1989) Description of the radiation scheme in the ECMWF model. ECMWF technical memorandum. 165. European Centre for Medium Range Weather Forcasts, Reading

MONRE (Ministry of Natural Resources and Environment) (2009) climate change: sea level rise scenarios for Vietnam. MONRE, Hanoi

Nakicenovic N, Alcamo J, Davis G, de Vries B and others (2000) IPCC special report on emissions scenarios. Cambridge University Press, Cambridge

Nguyen KC, Katzfey J, McGregor JL (2012) Global 60 km simulations with the CCAM: evaluation over the tropics. Clim Dyn 39:637–654

Nordeng TE (1994) Extended versions of the convective parametrization scheme at ECMWF and their impact on the mean and transient activity of the model in the tropics. ECMWF technical memorandum 206, European Centre for Medium Range Weather Forecasts, Reading

Phan VT, Ngo-Duc T, Ho TMH (2009) Seasonal and interannual variations of surface climate elements over Vietnam. Clim Res 40:49–60

Piani C, Weedon GP, Best M, Gomes SM, Viterbo P, Hagemann S, Haerter JO (2010) Statistical bias correction of global simulated daily precipitation and temperature for the application of hydrological models. J Hydrol (Amst) 395:199–215

Rauscher SA, Seth A, Liebmann B, Qian JH, Carmargo SJ (2007) Regional climate model-simulated timing and character of seasonal rains in South America. Mon Weather Rev 135:2642–2657

Rayner NA, Parker DE, Horton EB, Folland CK and others (2003) Global analyses of sea surface temperature, sea ice, and night marine air temperature since the late nineteenth century. J Geophys Res 108(D14):4407, doi:10.

1029/2002JD002670

Rockel B, Castro CL, Pielke RA, von Storch H, Leoncini G (2008) Dynamical downscaling: assessment of model system dependent retained and added variability for two different regional climate models. J Geophys Res 113: D21107, doi:10.1029/2007JD009461

Roeckner E, Arpe K, Bengtsson L, Christoph M and others (1996) The atmospheric general circulation model ECHAM4: model description and simulation of present-day climate. Report No. 218, Max-Planck-Institut für Meteorologie, Hamburg

Roeckner E, Bäuml G, Bonaventura L, Brokopf R and others (2003) The atmospheric general circulation model ECHAM5. I. Model description. Report No. 349. Max-Planck-Institut für Meteorologie, Hamburg

Schwarzkopf MD, Fels SB (1991) The simplified exchange method revisited: an accurate, rapid method for computation of infrared cooling rates and fluxes. J Geophys Res 96:9075–9096

Sen PK (1968) Estimates of the regression coefficient based on Kendall's Tau. J Am Stat Assoc 63:1379–1389

Seth A, Rauscher SA, Carmago SJ, Qian JH, Pal JS (2007) RegCM3 regional climatologies using reanalysis and ECHAM global model driving fields. Clim Dyn 28: 461–480

Solomon S, Qin D, Manning M, Chen Z and others (eds) (2007) Climate change 2007: the physical science basis. Contribution of Working Group I to the Fourth Assessment Report of the Intergovernmental Panel on Climate Change. Cambridge University Press, Cambridge

Tadross M, Jack C, Hewitson B (2005) On RCM-based projections of change in southern African regional climate. Geophys Res Lett 32:L23713, doi:10.1029/2005GL024460

Takahashi HG (2011) Long-term changes in rainfall and tropical cyclone activity over South and Southeast Asia. Adv Geosci 30:17–22

Tebaldi C, Knutti R (2007) The use of the multi-model ensemble in probabilistic climate projections. Philos Trans R Soc Lond A 365:2053–2075

Tiedtke M (1989) A comprehensive mass flux scheme for cumulus parameterization in largescale models. Mon Weather Rev 117:1779–1800

UNFCCC (2007) Climate change: impacts, vulnerabilities and adaptation in developing countries. United Nations Framework Convention on Climate Change, Climate Change Secretariat (UNFCCC), Bonn

Van der Linden P, Mitchell JFB (eds) (2009) ENSEMBLES: climate change and its impacts: summary of research and results from the ENSEMBLES project. Met Office Hadley Centre, Exeter

Wilby RL, Wigley TML, Conway D, Jones PD, Hewitson BC, Main J, Wilks DS (1998) Statistical downscaling of general circulation model output: a comparison of methods. Water Res 34:2995–3008

Wilby RL, Charles SP, Zorita E, Timbal B, Whetton P, Mearns LO (2004) Guidelines for use of climate scenarios developed from statistical downscaling methods: supporting material. Task Group on Scenarios for Climate Impact Assessment of the Intergovernmental Panel on Climate Change, Geneva

Yen MC, Chen TC, Hu HL, Tzeng RY, Dinh DT, Nguyen TTT, Wong CJ (2011) Interannual variation of the fall rainfall in central Vietnam. J Meteorol Soc Jpn 89A: 259–270

Editorial responsibility: Oliver Frauenfeld, College Station, Texas, USA

Submitted: July 19, 2012; Accepted: April 14, 2014
Proofs received from author(s): July 11, 2014